6th International Conference
on
Wind Turbine Noise

Glasgow 20-23 April 2015

Wind Turbine Noise Propagation – Results of Numerical Modelling Techniques to Investigate Specific Scenarios

Jonathan Sims, Andrew Bullmore, Hoare Lea Acoustics, 140 Aztec West Business Park, Bristol, BS32 4TX, UK. +44 1454 201 020, JonathanSims@hoarelea.com

Timothy van Renterghem, University of Ghent, B-9000 Gent, Belgium

Kirill Horoshenkov, University of Sheffield, Sheffield S10 2TN, UK

1. Introduction

The modelling of noise propagation from wind farms generally represents one of the key elements of planning assessments for such developments. Whilst no single calculation methodology has been standardised internationally, nationally adopted methodologies tend to utilise 'engineering' type models [Leventhall and Bowdler, 2011].

In the UK it is common to use the ISO 9613-2 [International Standards Organization, 1996] despite the fact that current commercial scale wind turbines clearly fall outside the stated scope of applicability of this standard, both in terms of source heights and the typical source to receiver separation distances that are of interest. In order to make ISO9613-2 usable for wind turbine noise, in the UK certain empirical adaptations based on field observations are made to the standardised calculation procedure. These adaptations are summarised in a good practice guide for the assessment of wind turbine noise issued by the UK Institute of Acoustics [Institute of Acoustics, 2013].

The objective of this paper is to investigate the potential merits of applying numerical propagation modelling techniques (and in particular the selected Green's Function Parabolic Equation - GFPE - calculation procedure) to wind turbine noise. It is believed that numerical modelling techniques could be used to supplement significantly, and ultimately might even supersede, the current use of 'engineering' models for day-to-day modelling of wind turbine noise. This is because the application of advanced numerical modelling techniques permits insight into propagation effects that may occur under quite specific conditions, thereby leading to

a greater understanding of the strengths and limitations of engineering models such as ISO 9613-2.

Despite considerable recent progress in the use of numerical methods it still remains a significant challenge to accurately predict wind turbine noise propagation into nearby residential areas in the presence of more extreme and/or varying environmental conditions. Typical numerical models which can be used to predict sound propagation from wind turbines are based on geometrical acoustics (e.g. [Li, 1996] or [Plovsing, 2011], fast field programme (FFP) (e.g.[Raspet, 1995]) and parabolic equation (PE) methods (e.g. [Kaliski, 2011] and [Forssén, 2010]). These and other models have been used in the past to investigate the ability of engineering models to predict the levels of wind turbine noise in the presence of a moving and inhomogeneous atmosphere and complex terrain. Typical engineering models which were used in these studies include Harmonoise [Harmonoise, 2011] and the aforementioned ISO 9613-2. These studies show that considerable discrepancies in the predicted noise levels can be observed when propagation conditions are more complex than can be accounted for in the engineering model (e.g. due to specific meteorological conditions) or when conditions are changing in time.

Engineering methods are generally derived from a combination of physical considerations and empirical observations. Their outputs generally reflect what is experienced in practice within the bounds of the assumed propagation conditions. As a simple example, the ISO9613-2 model has been developed based on observations of received noise levels that occur under downwind conditions or conditions of a moderate temperature inversion, which are both conditions that lead to higher received noise levels than would be expected under other meteorological conditions. Consequently the model would be expected to over-estimate received noise levels under upwind or unstable conditions.

Whilst the use of ‘simple’ engineering methods to derive results for specific scenarios is highly useful, and particularly so for predicting received noise levels towards the extremes of the ranges of levels that may occur in practice, there are increasingly good reasons to revisit such applications. First, as the study of cumulative noise from neighbouring wind farms becomes increasingly relevant, more emphasis is being placed on the differences between upwind, crosswind and downwind propagation scenarios. Second, issues can arise relating to propagation across variable terrain and under meteorological conditions that fall outside the basic engineering model assumptions made. In the specific case of the ISO 9613-2 model examples include propagation over valleys, over larger distances, over large bodies of water, or propagation under specific meteorological conditions that give rise to extreme or complex sound speed gradients.

Such scenarios require more detailed modelling techniques to be employed if the effects of the specific features of interest are to be quantified. This paper discusses the numerical modelling of several scenarios using a GFPE method in order to establish the adequacy and/or limitations of the ISO 9613-2 method in these cases. Unlike previous research, this work makes use of the axisymmetric GFPE method to study sound propagation from a large wind turbine over a long range of up to 2 km or more. The efficient implementation of this GFPE method allows the calculation of results in terms of overall A-weighted noise levels and not, as has been common in the past, in terms of individual or band limited frequencies.

2. Details of the GFPE model

The GFPE method used in this paper [Gilbert, 1993] [Salomons, 1998] utilises a highly efficient approach to solve the parabolic equation, simulating one-way sound propagation away from the source. The GFPE is especially efficient as it allows large step sizes in the propagation direction. These horizontal step sizes are limited by the inhomogeneity of the atmosphere rather than by the sound wavelength. In the implementation reported here, stepping was performed at 10 times the wavelength with a maximum step size of 10 m to ensure sufficient spatial resolution when plotting results. In the vertical direction, however, a considerably finer spatial discretisation of one tenth of a wavelength is needed.

The effective sound speed profiles may contain both upward and downward refracting parts and may be range-dependent. Locally reacting, range-dependent impedance planes can be used to model reflection from the ground. Given the large propagation distances considered in this paper, the angle limitation arising from the parabolic equation approximation is not an issue, even for an elevated source like a wind turbine.

The GFPE results presented in this paper have been based on the following general assumptions:

- all calculations model a single point source, therefore no account is taken of source directivity or interference between multiple sources;
- all calculations assume propagation over a perfectly flat horizontal plane, therefore no account is taken of variations in terrain height;
- all calculations assume that both atmospheric conditions and ground conditions remain constant along the horizontal axis; and
- no account has been taken of atmospheric turbulence (for the cases of upwind propagation the effect of atmospheric turbulence has been approximated by limiting shadow zone attenuation).

Whilst the above assumptions are simplifications, the model has been kept deliberately simple in order to reveal the influence of specific aspects of wind turbine sound propagation in isolation from other effects. The assumptions thus allow the outputs of the GFPE calculations to be meaningfully compared with the output of engineering-type models in relation to propagation effects only. In this regard, whilst the GFPE method necessarily produces detailed frequency dependant information, all results presented in this paper are interpreted on the basis of the resultant calculated overall A-weighted noise levels only.

3. Results of GFPE modelling

3.1 General calculation parameters

The situations considered herein are concerned primarily with propagation effects and how variations in the sound propagation path due to both meteorological and ground conditions may cause received sound pressure levels to vary as a function of distance from the source. For this reason the source has been consistently modelled

as an omnidirectional point source with the sound power output spectrum as presented in Table 1. This spectrum is representative of a typical 2 MW to 3 MW wind turbine at rated power, where rated power tends to occur at a hub height wind speed of around 11 m/s.

	Octave band centre frequency, Hz								**dB(A)**
	63	125	250	500	1000	2000	4000	8000	
SWL, dB(A)	90	95	100	99	96	97	92	79	**105.0**

Table 1 – Modelled source sound power output (A-weighted octave band spectrum) for all GFPE and ISO9613-2 calculations reported in this paper[1].

Except where stated otherwise, the source is modelled at a height of 80 m above ground level. In all cases the receiver (i.e. the noise immission calculation point) is located at 4 m height. Since this paper is concerned with propagation effects rather than variations due to changes in source sound power levels, in those cases where predictions have been produced for source heights other than 80 m the same sound power levels as shown in Table 1 above have been consistently adopted. This approach allows for the meaningful direct comparison of results because any differences in the calculated received noise levels can be attributed solely to the propagation path. Calculations are generally reported at receiver distances of up to 2 km from the source, although in some cases further distances are considered. This baseline propagation scenario is shown schematically in Figure 1.

[1] The UK IoA GPG [IoA, 2013] recommends that a source uncertainty margin of typically +2 dB is added to the measured sound power output of turbines prior to input to the ISO 9613-2 calculation procedure when applied to wind turbine noise. All results presented herein have adopted the sound power levels as listed in Table 1 without the addition of any margin for either the GFPE or the ISO 9613-2 calculations in order to allow the direct comparison of results on the basis of propagation effects alone.

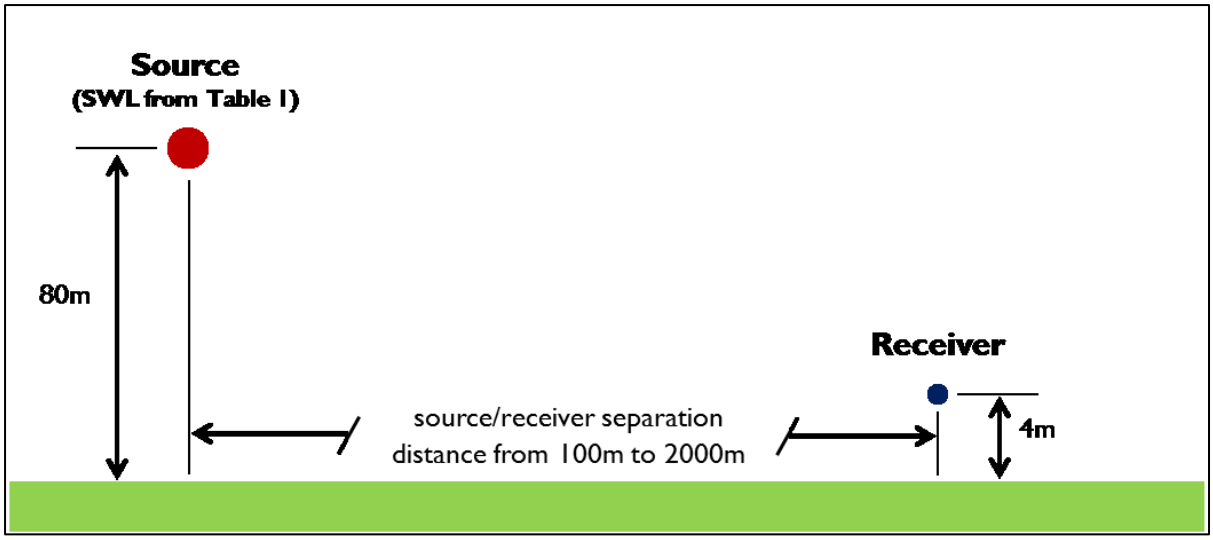

Figure 1. Schematic of the baseline modelled scenario

The (effective) sound speed profiles used in the models are governed by two factors: the temperature gradients and the wind speed gradients. Temperature profiles and wind speed profiles outdoors are linked and this is achieved by applying the Monin-Obukhov similarity theory (MOST), assuming either an unstable, neutral or stable atmosphere. These three stability conditions have been characterised by a Monin-Obukhov length L_{mo} of -100 m, infinity, and 100 m, respectively. For the unstable atmosphere the Businger-Dyer relations have been used, whilst for a stable atmosphere the Businger-Dyer relations [Dyer, 1974] have been used for the case of $z/L_{stable} \leq 0.5$ and the Holtslag relations [Holtslag, 1984] for $z/L_{stable} > 0.5$, where z is the height above the ground. All data is referred to a wind speed of 11 m/s at a height of 80 m, thereby corresponding to the source spectrum provided in Table 1. A roughness length z_0 = 0.05 m has been used. In all cases a temperature lapse has been modelled based on a ground surface temperature of $T_{surface}$ = 283 K and a standard atmospheric temperature lapse rate of -6.5K/km, as shown in Figure 2.

The resultant wind shears are shown as the solid lines in Figure 3. Also shown in Figure 3 as the dashed lines are the corresponding power law wind speed profiles (for this specific z_0 = 0.05 m) with shear exponents of $m_{unstable}$ = 0.102, $m_{neutral}$ = 0.150 and m_{stable} = 0.340.

The resultant calculated sound speed profiles for pure downwind propagation are obtained from combining the results of Figures 2 and 3, the results of which are shown in Figure 4.

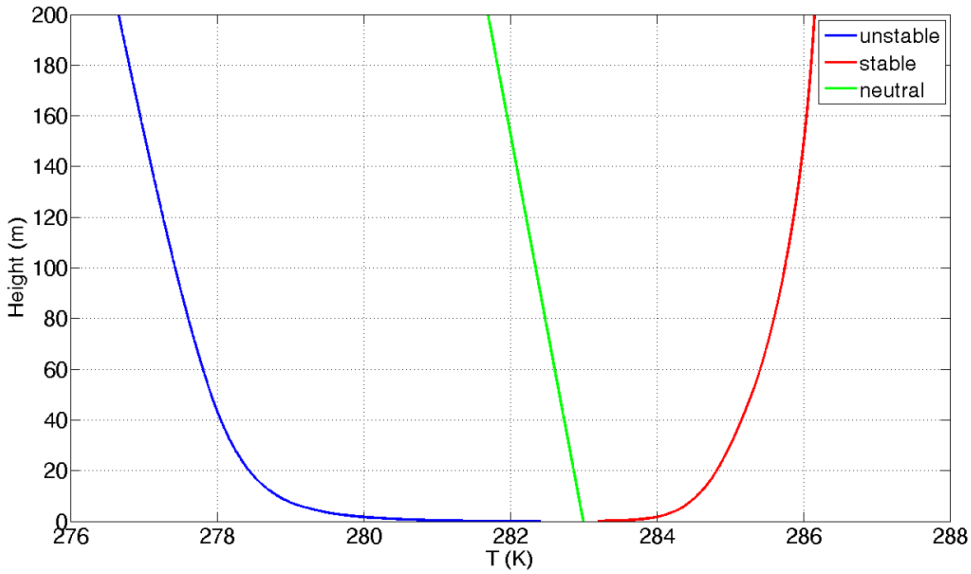

Figure 2. Temperature profiles for unstable, stable and neutral atmospheres used for the GFPE calculations in this paper. See text for overview of parameters.

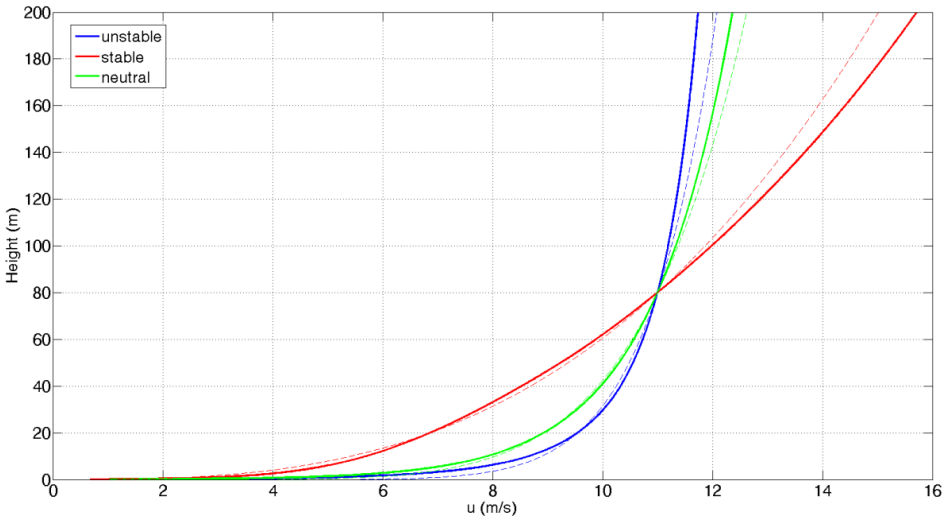

Figure 3. Wind speed profiles for an unstable, stable and neutral atmosphere used for the GFPE calculations in this paper. The profiles using MOST theory are indicated with the full lines, the corresponding best fitting power-law wind speed functions are depicted with the dashed lines. See text for overview of parameters.

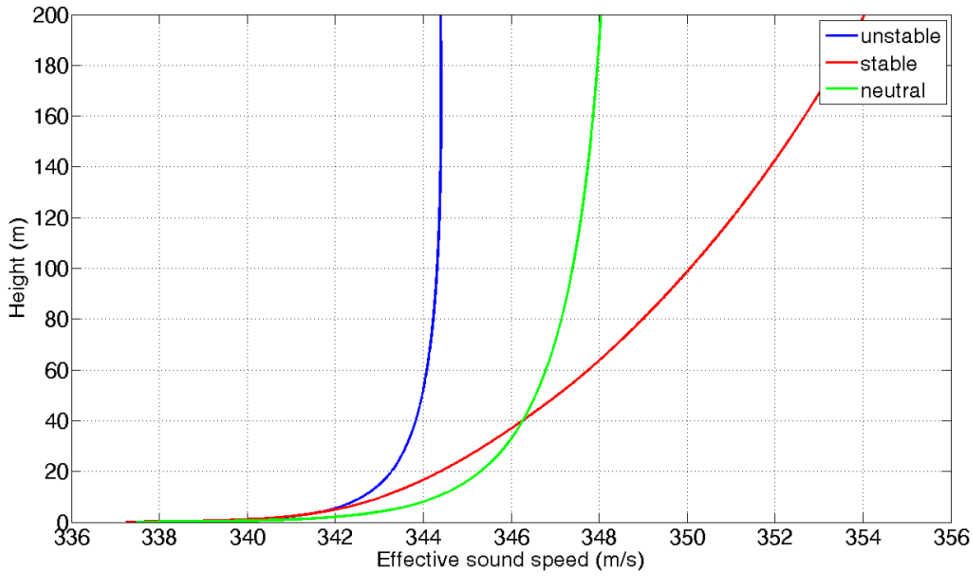

Figure 4. Effective sound speed profiles used for the GFPE calculations in this paper. Pure downwind sound propagation is considered.

The effective sound speed gradients can also be calculated for non-downwind conditions. Figure 5 shows the results of these calculations for 30 degree wind direction increments ranging from fully downwind of the source (the most extreme positive sound speed gradient) to fully upwind of the source (the most extreme negative sound speed gradient). In Figure 5 the same wind speed at the source height of u_{80m} = 11 m/s applies for all wind direction angles.

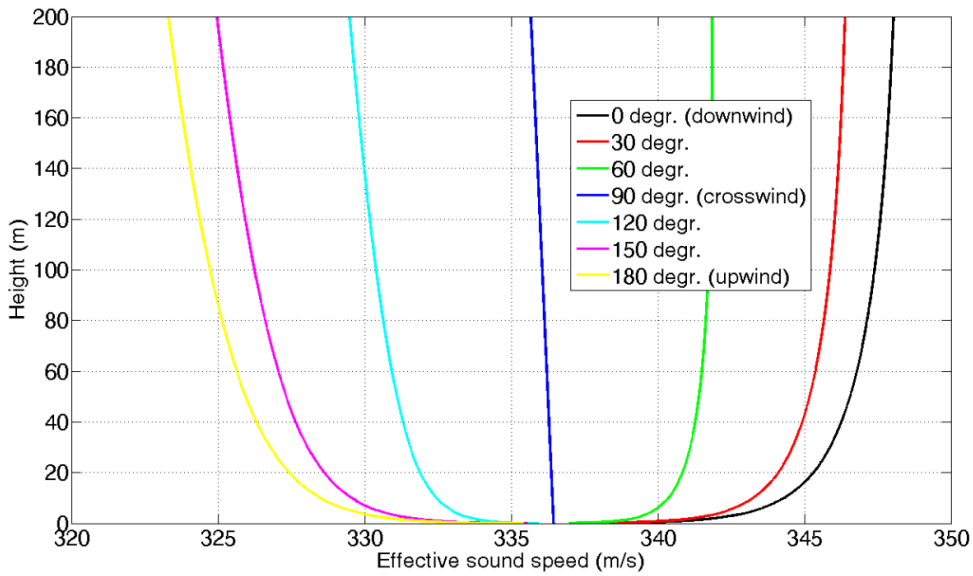

Figure 5. Effective sound speed profiles used for the GFPE calculations in this paper

for a range of wind directions from purely downwind (0 degrees) up to purely upwind (180 degrees) in 30 degree increments. A neutral atmosphere is simulated.

Ground impedance has been incorporated into the GFPE models using the Delany and Bazley frequency-dependent impedance model [Delany and Bazley, 1970] with a flow resistivity of 150 kPa/m^2 for grass/pasture/farm land and 15 kPa/m^2 for snow, as suggested in the HARMONOISE engineering prediction model [Nota et al, 2005]. Fully rigid or hard ground is modelled by setting the reflection coefficient of the ground plane to 1.

3.2 Convergence of the GFPE model in calculating octave band and overall A-weighted levels

One consideration relating to the practical adoption of PE modelling techniques is that for each run the model yields results corresponding to a single frequency only. Whilst such single frequency results may be instructive in understanding the principles of certain propagation effects, the practical impact of wind turbine noise is more generally judged not on the basis of single frequencies but on broader band stimuli, and most often the overall A-weighted level of noise. This consideration therefore raises the question as to whether or not PE models can be used to generate overall A-weighted noise levels, or whether the calculation overheads are so great that their practical use is presently restricted solely to the calculation of more restricted bandwidths at lower frequencies.

In answering this, two key issues need to be addressed:

- what range of frequencies would need to be included in any calculation in order for the overall A-weighted noise level to converge?
- how many individual single frequency components are required to be included across the selected frequency range for their sum to converge?

An initial estimate of the required range of frequencies can be usefully established from the ISO9613-2 calculation procedure. Inputting the selected source and propagation parameters to this procedure (with G = 0.5, T = 15 degC, RH = 70%) for the two propagation distances of 1000 m and 2000 m yields the results presented in Tables 2.

Table 3 shows the results of summing the calculated individual octave band levels from Table 2, starting from 63 Hz upwards. Convergence towards the overall A-weighted noise levels at both distances occurs to within one decimal place by including up to the 2000 Hz octave band inclusive.

	Octave band centre frequency, Hz								**dB(A)**
	63	125	250	500	1000	2000	4000	8000	
SPL @ 1000 m	21.6	23.1	28.0	27.3	22.8	18.0	-10.4	-107.8	**32.5**
SPL @ 2000 m	15.4	16.7	21.0	19.3	13.2	4.0	-49.1	-230.4	**25.0**

Table 2 – Octave band and overall A-weighted noise levels calculated using the ISO9613-2 calculation methodology at source to receiver separation distances of 1000m and 2000m. See text for overview of parameters.

	Octave band centre frequency, Hz								dB(A)
	63	125	250	500	1000	2000	4000	8000	
SPL @ 1000 m	21.6	25.4	29.9	31.8	32.3	32.5	32.5	32.5	**32.5**
SPL @ 2000 m	15.4	19.1	23.2	24.7	25.0	25.0	25.0	25.0	**25.0**

Table 3 – Effect of summing the individual octave band levels from Table 2 starting at 63 Hz upwards, showing that the octave bands up to and including 2000 Hz are required for convergence to the overall A-weighted level to within one decimal place.

In addition to the foregoing results showing the convergence of the overall A-weighted noise level, consideration has also been given to the number of individual frequencies required to ensure convergence in each octave band. In a preliminary test a convergence study revealed that 30 individual sound frequencies would be sufficient for each octave band of interest.

On the conservative interpretation of the foregoing results, all overall A-weighted results presented in this paper have been calculated using the summation of 30 individual frequency components in each of the octave frequency bands from 63 Hz to 2000 Hz inclusive. The sound power levels in each of the octave bands has been modelled as per Table 1 and evenly distributed across the 30 individual calculation frequencies making up each octave band.

3.3 Comparison of GFPE results with ISO9613-2 results

Prior to investigating the effects on propagation of specific conditions it is useful to compare the outputs of the GFPE method against the specific implementation of the ISO9613-2 method adopted for the calculation of wind turbine noise immissions in the UK [Institute of Acoustics, 2013]. The results of the ISO9613-2 method are commonly stated as relating to the typical upper levels of noise immission that may be experienced in practice, such as may occur in the case of a downwards refracting atmosphere under downwind and/or temperature inversion conditions.

Figure 6 shows the results of the GFPE calculations for the baseline scenario of Figure 1 with propagation over grass land (flow resistivity = 150 kPa/m^2). Also shown overlaid in Figure 6 are the results of the ISO9613-2 method, obtained by adopting the same baseline parameters shown in Figure 1 and a common ground factor of G=0.5 for the source, middle and receiver regions[2]. Results are shown for the three

[2] In all cases where the results of ISO 9613-2 calculations are reported in this paper, the stated ground factor value, G, has consistently been applied to all three propagation regions.

downwind cases of neutral, stable and unstable atmospheric wind speed profiles, as previously shown in Figure 3.

Figure 7 shows the corresponding GFPE results using the same baseline parameters of Figure 1 but now for the case of propagation over rigid ground. Overlaid in Figure 7 are the results of equivalent ISO9613-2 predictions assuming a ground attenuation factor of G=0 (equivalent to hard ground) and G=0.5.

The results shown in Figures 6 and 7 reveal the relatively small (less than 1 dB(A)) atmospheric refractive effects for the case of such an elevated source height under downwind conditions. This finding is consistent with the results of practical measurements on operational wind farms, including under differing site measured wind shear conditions [Cooper and Evans, 2013] [Cooper et al, 2014]. The results also illustrate the agreement between the GFPE model outputs and those of ISO9613-2.

The following Figure 8 presents a comparison of GFPE predictions for various different ground impedances (corresponding to rigid ground, grass, snow and sand with varying moisture content) against the ISO 9613-2 predictions with G=0 and G=0.5.

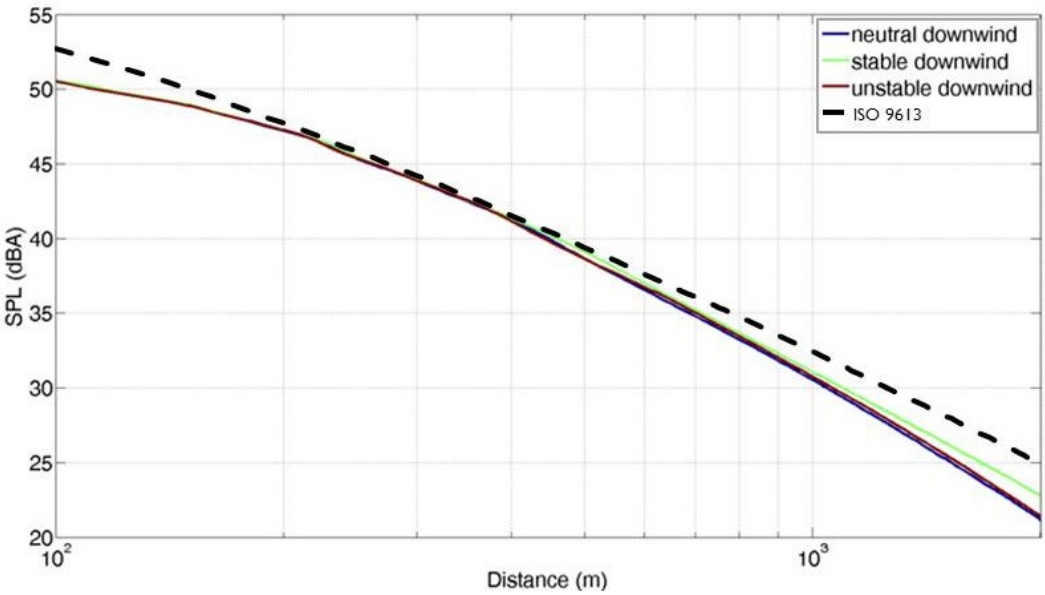

Figure 6. Results of the GFPE calculations for the baseline scenario of Figure 1 with propagation over grass land (flow resistivity = 150 kPa/m^2 for the three separate cases of a neutral, unstable and stable atmosphere. Also shown as the dashed line is the calculation undertaken in accordance with ISO9613-2 assuming G=0.5 for all propagation regions.

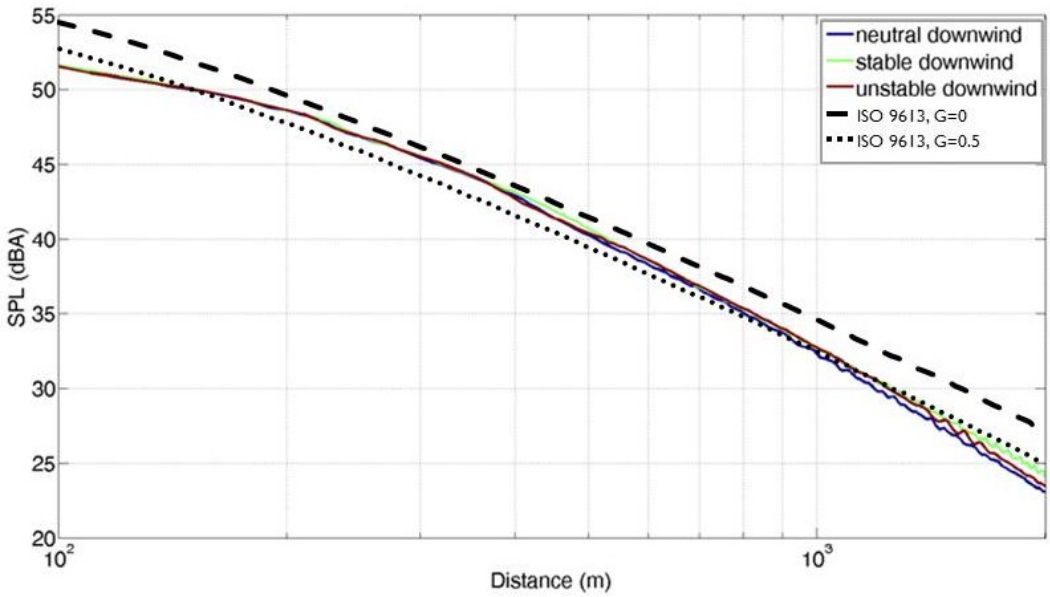

Figure 7. Results of the GFPE calculations for the baseline scenario of Figure 1 with propagation over rigid ground for the three separate cases of a neutral, unstable and stable atmosphere. Also shown are the calculations undertaken in accordance with ISO9613-2 assuming G=0 for all propagation regions (dashed line) and with G=0.5 for all propagation regions (dotted line).

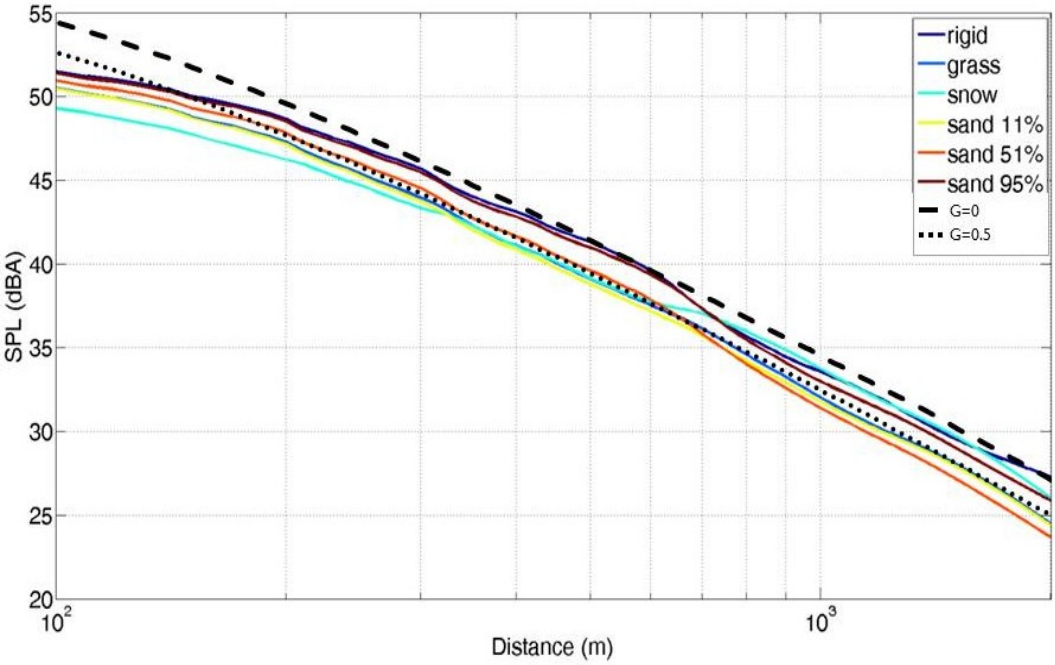

Figure 8. Results of the GFPE calculations for the baseline scenario of Figure 1 with propagation over different ground types. Also shown are the corresponding calculations undertaken in accordance with ISO9613-2.

3.4 The effect of source height

Whilst the present paper is focussed on establishing propagation effects associated with larger scale commercial wind turbines, the insensitivity of the preceding results to both ground and refraction effects may at first sight be unexpected. The effect has been checked by repeating the calculations but for a lower source height of 10 m above ground level (but with an identical source power spectrum as per Table 1). Reference to Figure 4 reveals that the reduction in source height from 80 m to 10 m results in the source radiating energy into a region of significantly enhanced sound speed gradients.

Figure 9 shows the differences in received noise levels for the case of a 10 m height source with sound propagation over the three scenarios of rigid ground, grassland and snow, all of these cases being calculated for conditions of no atmospheric refraction. In this case of a 10 m source height the effect of the rigid ground on the received noise levels is quite apparent beyond approximately 250 m from the source. Figure 10 shows the corresponding 10 m source height results but adding in the effect of downwards refraction under the condition of neutral atmospheric stability.

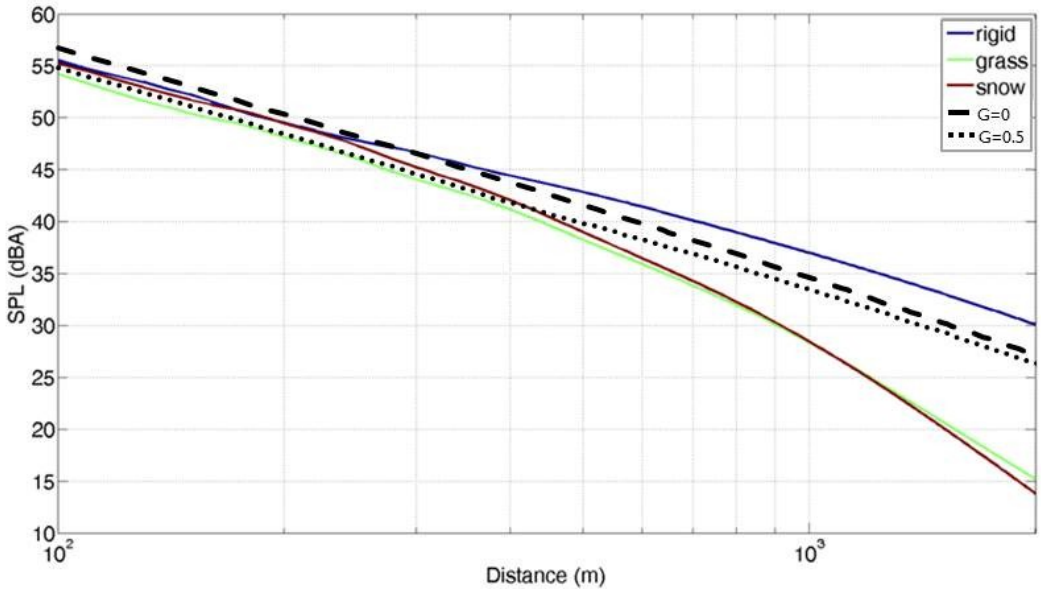

Figure 9. Received noise levels for the case of a 10 m height source with sound propagation over rigid ground, grassland and snow, all of these cases being calculated for conditions of no atmospheric refraction. Also shown are the corresponding calculations undertaken in accordance with ISO9613-2.

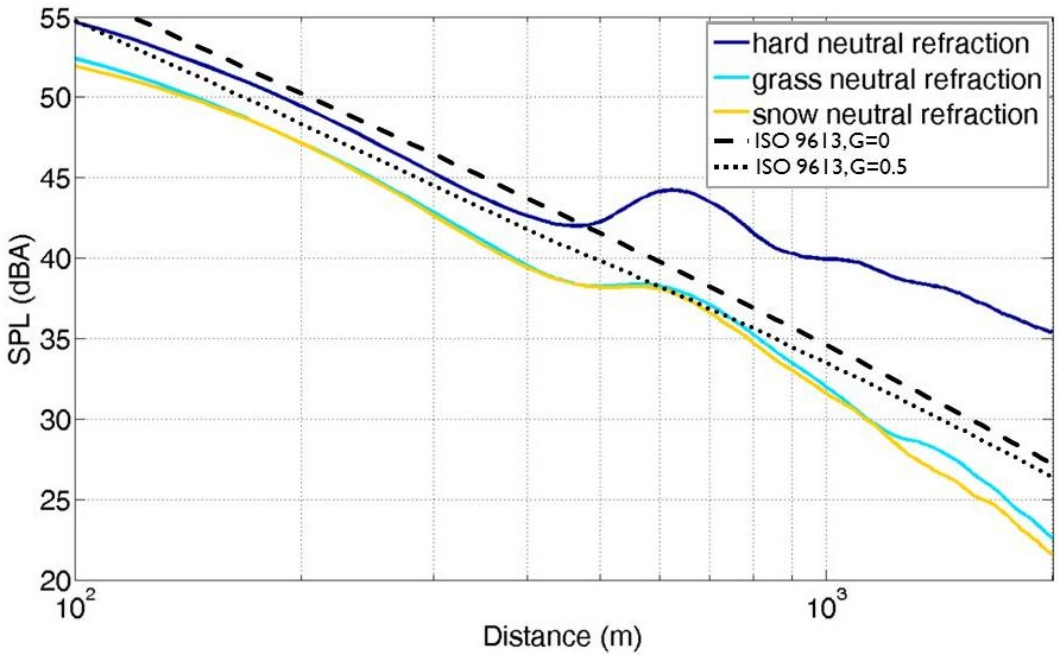

Figure 10. Received noise levels for the case of a 10 m height source with sound propagation over rigid ground, grassland and snow, all of these cases being calculated for conditions of atmospheric refraction in a neutral atmosphere. Also shown are the calculations undertaken in accordance with ISO9613-2.

A clearer direct comparison of the effect of atmospheric refraction for different source heights can be seen in the results of Figure 11 in which the results for 10 m and 80 m source heights are directly compared. These results show that, at longer distances, the atmospheric conditions influence significantly the calculated received noise levels for propagation over rigid ground for the 10 m source height (z_s). This variation is between approximately 10 dB to 15 dB. Similarly large positive variations are not evident in the results for the 80 m source height. Interestingly, for the case of an 80 m source height the presence of a downwards refracting atmosphere leads to less divergent, and even slightly lower, calculated far field noise levels than is the case with no refraction, whereas for a 10 m source height the opposite is true. Note that the GFPE predictions presented in Figure 9 assume a neutral atmosphere, whereas the GFPE predictions presented in Figure 10 assume a stable atmosphere, hence the slight differences in the GFPE results between the two figures.

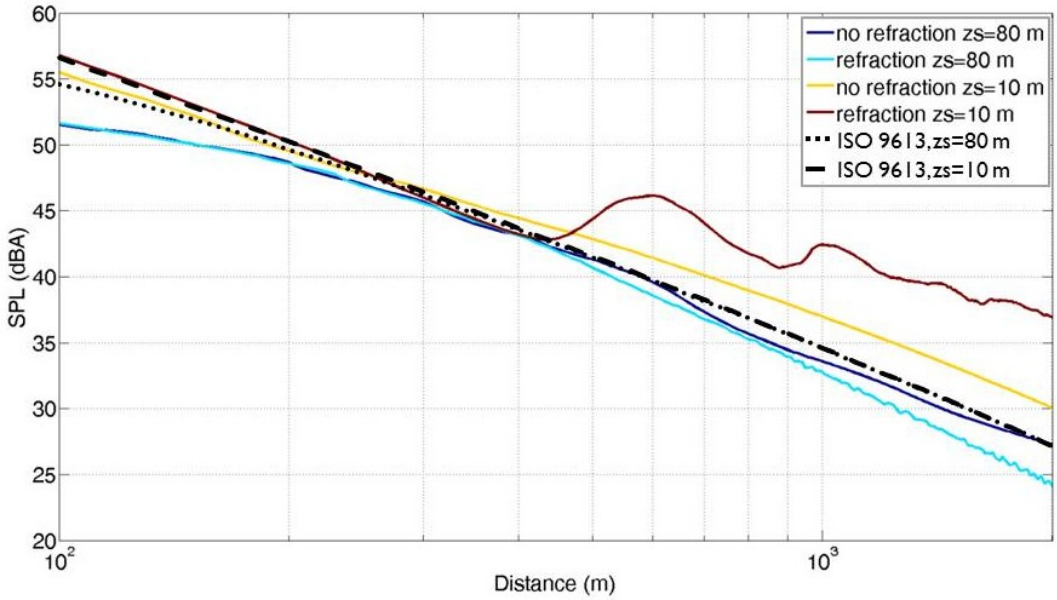

Figure 11. Comparison of received noise levels for the case of both a 10 m and an 80 m height source with sound propagation over rigid ground for the two cases of no refraction and refraction in a stable atmosphere. Also shown are the corresponding calculations undertaken in accordance with ISO9613-2 with G=0.

The preceding discussion has illustrated the relative insensitivity to received sound pressure levels to atmospheric stability when considering an 80 m source height, which was specifically selected as being typical of the hub height of a large scale wind turbine. However, the effect of source height may become relevant for wind turbine sound, even for a turbine of this size, if more detailed consideration is given to the actual height of the sources on that turbine as opposed to the common modelling assumption made of a point source at hub height. This assumption largely derives from the determination of the effective sound power output of such turbines in accordance with the IEC61400-11 procedure [IEC 61400-11, 2013] which assumes that the effective source location is collocated with the hub of the turbine. It is well established that the measured overall noise from such turbines is generally dominated by so-called trailing edge aerodynamic noise, which tends to be prevalently generated towards the outer radius of each blade [Oerlemans and Schepers, 2009]. The following Figure 12 shows the situation for a turbine with a hub height of 80 m and a rotor diameter of 90 m. The two illustrations show the effective trailing edge source locations for the two extreme rotor positions.

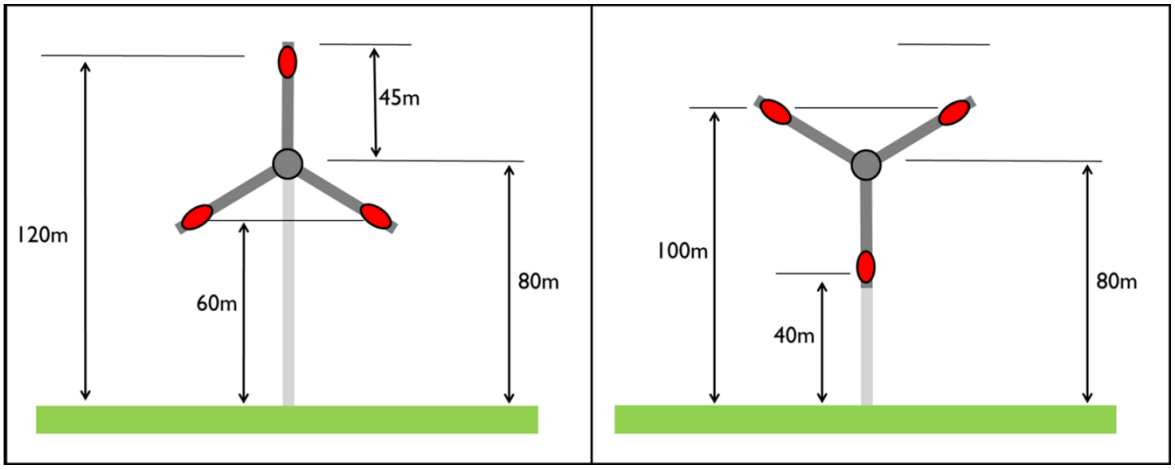

Figure 12. Schematic diagram showing the approximate locations of the dominant trailing edge aerodynamic noise sources for two opposing rotor positions.

In the case illustrated in Figure 12, the effective source height may vary between approximately 40 m and 120 m. Figures 13a and 13b shows the results of GFPE calculations undertaken for each of the various source heights shown in Figure 12 for downwind conditions in unstable and stable atmospheres respectively. For the purpose of enabling the direct comparison of results, the source sound power attributed to each source height is again that presented in Table 1. In practice the overall sound power reported for a turbine will result from the cumulative effects of contributions of each of the three blades. A lower sound power level than listed in Table 1would therefore be emitted from each of the individual blades. In the idealised case that an equal sound power was emitted from each blade, regardless of its rotational location, this would result in each of the modelled sources having a sound power level approximately 5 dB lower than that of Table 1.

As can be seen from Figure 13a, only slight variations in the received noise levels due to the different source heights is predicted beyond approximately 400m. The difference in the predicted noise levels slightly increases beyond this distance. This suggests that the modelling assumption of representing the turbine rotor by a point source at the hub centre is reasonable for horizontal distances greater than approximately 300 m from the turbine for the particular turbine dimensions considered here.

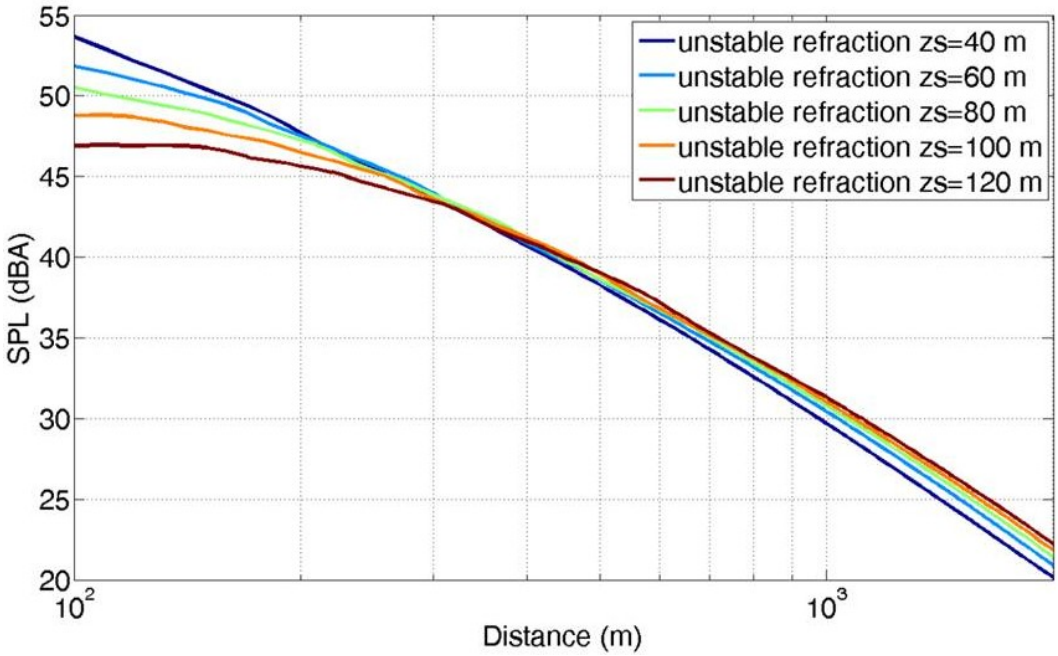

Figure 13a. The results of GFPE calculations undertaken for the various source heights shown in Figure 12, for downwind conditions with refraction in an unstable atmosphere.

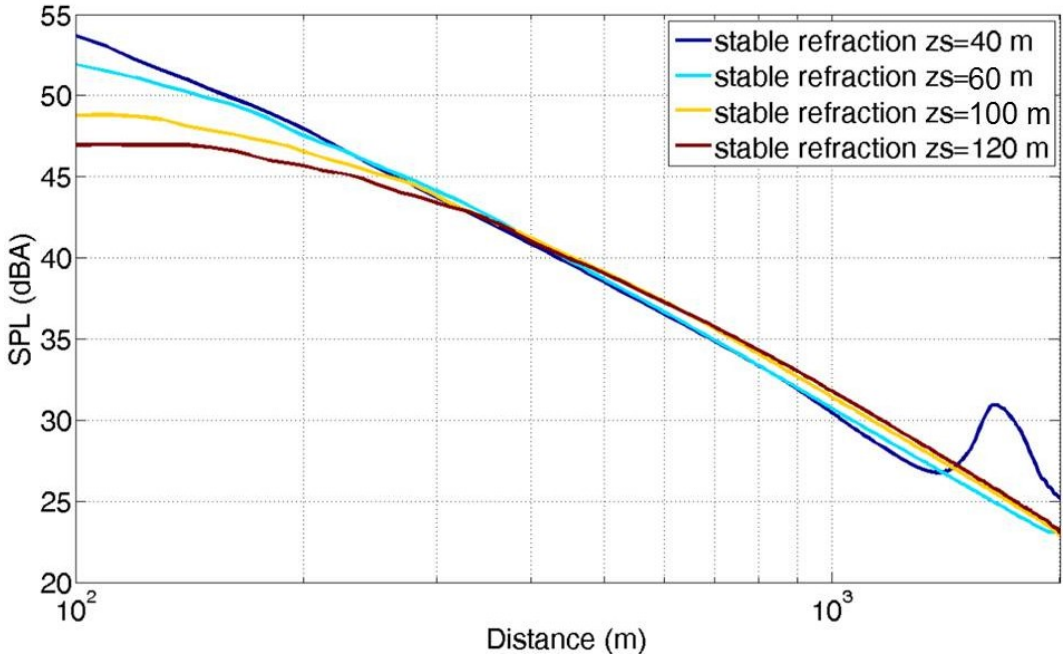

Figure 13b. The results of GFPE calculations undertaken for the various source heights shown in Figure 12, for downwind conditions with refraction in a stable atmosphere.

A turbine that is rotating will constantly be transitioning between the two configurations shown in Figure 12, in which the noise generating portion of two blades are at either approximately 60 m or 100 m above ground whilst the noise generating portion of the third blade is respectively either at 120 m or 40 m above ground. Consequently, there is the possibility that the received noise level, even at distances beyond 300m, may vary in level as the blades rotate due to the differing effects of propagation from the three trailing edge noise sources at their various sources heights.

This has been investigated at a receiver distance of 1 km by summing the contributions from each of the three blades to arrive at a total overall noise level corresponding to the two extremes of rotor positions shown in Figure 12. In both cases it is assumed that the total sound power level provided in Table 1 is evenly spread over the three turbine blades. Comparison of the calculated overall received noise levels between the two rotor positions indicates that the effects of propagation alone accounts for only 0.1 dB difference. This result indicates that, under the assumed conditions, propagation effects would result in an insignificant degree of amplitude modulation as the turbine blades rotate.

Previous research [ReUK, 2013] has suggested that one potential cause of amplitude modulated noise from wind turbines is an increase in the source sound power level for the blades as they pass through the top of the arc of rotation (i.e. corresponding to the source at a height of 120 m shown on the left of Figure 12). This increase is due to the blade entering partial stall. Figure 14 indicates the modified predicted received level differences between the two rotor positions shown in Figure 12 (again calculated by summing the calculated contributions of all three blades in each case) when it is assumed that the sound power of the uppermost (120 m height) source *only* is increased in level relative to the lower sources. Results are shown corresponding to an increase in source level for this uppermost source ranging from 1 dB up to 15 dB relative to the lower sources, all of which are modelled with the same, constant source level. In all cases the source has been maintained as an omnidirectional point source, thereby eliminating any of the radiation directivity effects otherwise associated with trailing edge sources [Oerlemans, 2009].

The calculated differences in received noise levels correspond to the depth of amplitude modulation shown in Figure 14 which may be introduced into the received noise level corresponding to the rotational rate of the source turbine. It should be noted that the results presented in Figure 14 have been derived on the basis of the addition of the overall A-weighted noise levels only. No account has been taken of any potential change in the source spectrum from that presented in Table 1 between the different blade positions.

Based on the results of Figure 14, a 3 dB modulation depth would require the sound power level of the upper source to increase by approximately 5 dB, with a 7 dB modulation depth resulting from a 10 dB increase in the sound power level of the upper source.

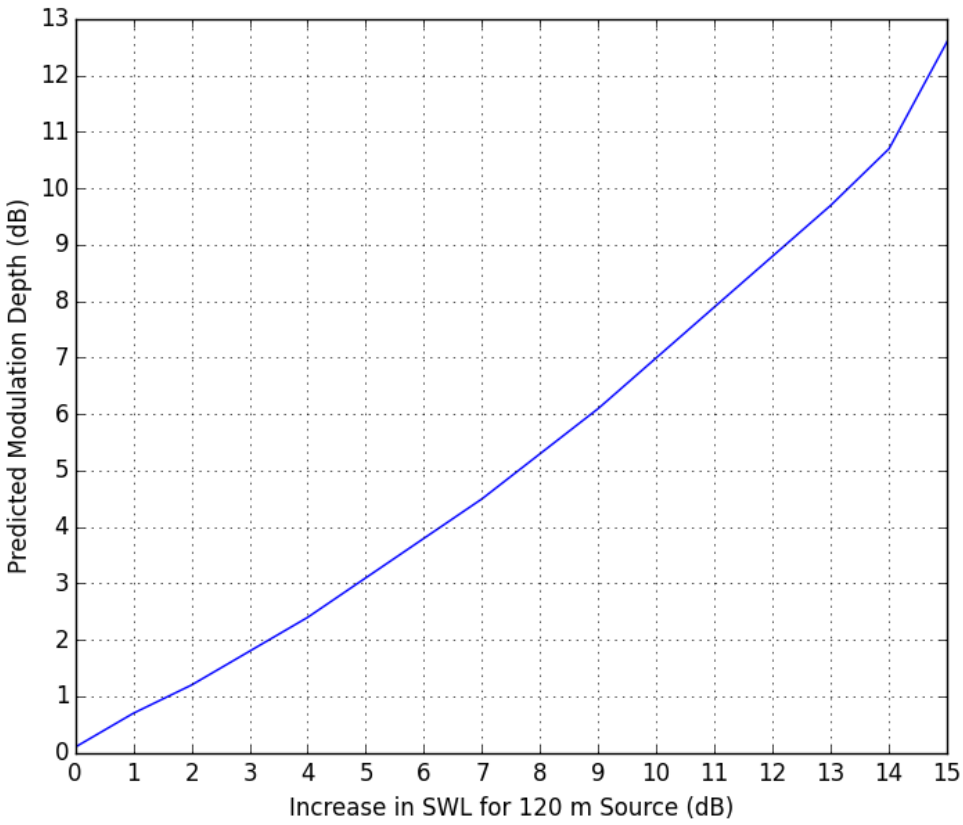

Figure 14. The predicted amplitude modulation depth at 1000 m distance from the source derived from the results of Figure 13a if the upper (120 m) blade source from Figure 12 is assumed to increase in source level by the stated amount relative to the lower height sources, which are all modelled as having the same, constant source level.

The preceding discussion on modulation has been based on the results presented in Figure 13a. However, an interesting feature can be seen in Figure 13b, which predicts an increase in level from a source at 40 m height at a horizontal distance of approximately 1.5 km from the source under stable atmospheric conditions. It should be noted that, with regard to modulation, this increase in noise level could act to increase or decrease the received modulation depth at distance depending on whether or not any part of the upper rotor is in stall. It should also be noted that the magnitude of this effect in real world situations would be modified to some degree by the presence of atmospheric turbulence, non-flat terrain profiles, varying ground conditions and varying atmospheric conditions along the propagation path. Such effects have not been included in the GFPE implementation considered here.

3.5 Effect of wind direction on sound propagation

Figure 5 presented the sound speed profiles relating to neutral atmospheric stability and standard temperature lapse conditions for the cases of multiple wind directions in 30 degree increments between downwind and upwind of the source.

Figures 15 show the results of introducing these sound speed profiles into the GFPE model for the baseline case of Figure 1 of an 80 m source height and noise propagation over flat grassland to a 4 m height receiver. The results of Figures 15 merit further discussion in respect of the upwind calculated noise levels. Based on consideration of basic ray theory it is the case that propagation in an upwind direction will result in the upwards refraction of sound. This means that, beyond some limiting point which is determined by the source height coupled with the strength of the upwards refraction, there will be a shadow region into which no sound energy can theoretically propagate. In reality, the presence of turbulence means that some sound energy 'leaks' past the limiting ray into the acoustic shadow zone.

In order to model this effect two methods are frequently adopted. The first is to undertake a Monte-Carlo simulation in the PE calculation with small perturbations being introduced into the sound speed profiles. This procedure effectively eliminates 'hard line' results, such as the existence of a distinct limiting ray, and in so doing replicates what would be experienced in practice as the atmosphere is naturally not truly homogeneous, either as a function of time or space. The second method simply recognises that atmospheric turbulence will always result in a practical limit to the reduction of noise levels in the shadow region. Common practice is that this limit should be set at -20 dB relative to the sound level that would be expected to occur under free field conditions [Salomons, 2001]. This second method is that which has been implemented in the results of Figure 15, which show for comparison the effects of limiting the shadow zone reduction to both -20 dB (moderate turbulence) in Figure 15(a) and -10 dB (strong turbulence) in Figure 15(b).

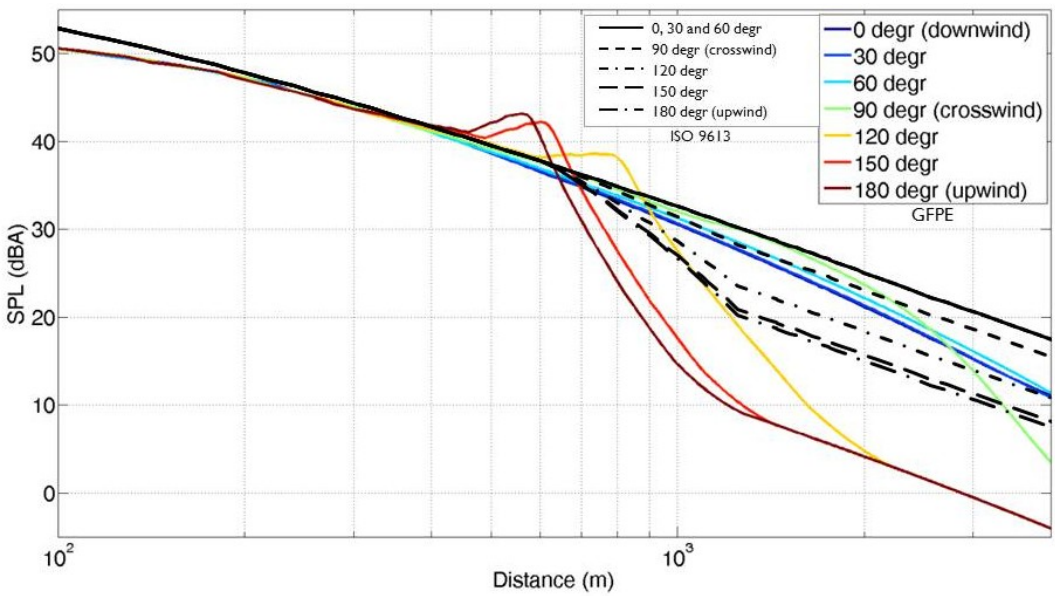

Figure 15(a) Predicted noise immission levels under varying wind directions. GFPE predictions shown as coloured lines, assuming neutral refraction, a surface impedance relating to grass and turbulent effects that limit shadow zone attenuation to -20 dB relative to free field. The corresponding ISO 9613-2 predictions assuming a ground factor of G=0.5 and accounting for directivity effects in accordance with the IoA GPG are shown as the black lines.

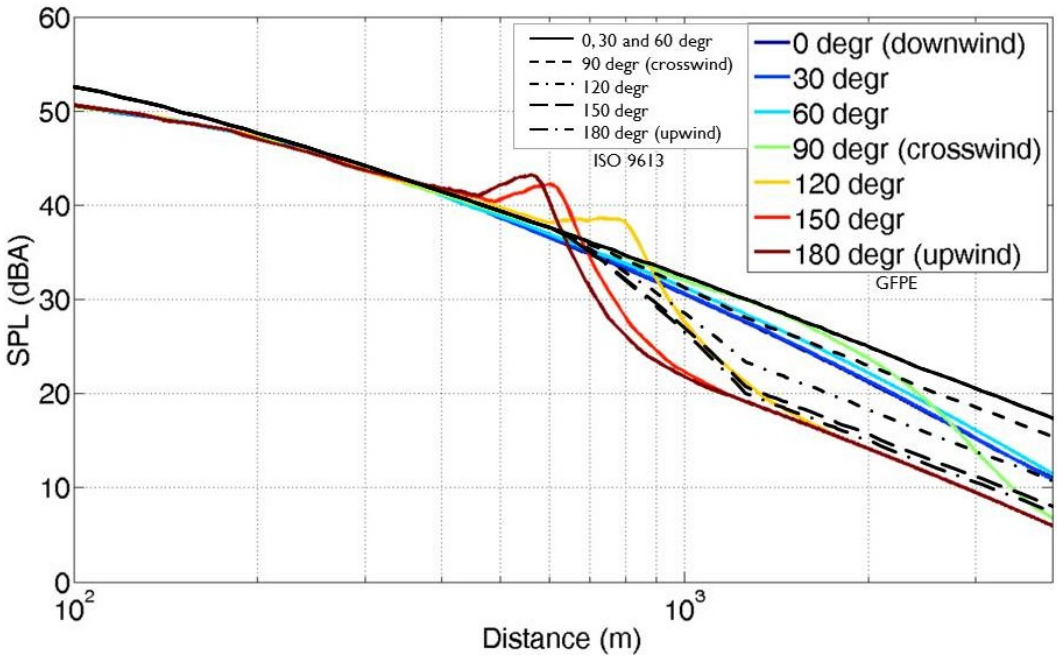

Figure 15(b) Predicted noise levels under varying wind directions. GFPE predictions shown as coloured lines, assuming refraction in a neutral atmosphere, a surface impedance relating to grass and turbulent effects that limit shadow zone attenuation to -10 dB relative to free field. The corresponding ISO 9613-2 predictions assuming a ground factor of G=0.5 and accounting for directivity effects in accordance with the IoA GPG are shown as the black lines.

Also shown in Figures 15 are the results obtained from applying wind directivity corrections recommended for adoption by the IoA GPG [IoA, 2013] when using the ISO9613-2 calculation procedure with G=0.5. These have been calculated based on the recommendation that there should be no upwind attenuation accounted for until a distance of 5 tip heights from the turbine (in this case 5 x 125 m = 625 m), with the upwind attenuation 'topping out' at maximum of approximately 10 dB at a distance of 10 tip heights from the turbine (in this case 10 x 125 m = 1250 m). In crosswind conditions a reduction of up to 2 dB is assumed, but no reduction is applied between downwind and 10 degrees from crosswind directions.

The observed increase in the sound pressure level beyond 500 m can be due to the refraction and multiple reflections of the sound wave emitted by the turbine which can cause caustics and interference. Expression (11.8) in [Attenborough et al, 2007] contains the terms $kR'_{1,2}$ and $\chi_{1,2}$, where k is the wavenumber in air, R'_1 is the path length for the direct sound, R'_2 is the path length for the ground reflection and $\chi_{1,2}$ are the corresponding phases in these waves at the point where they cause a caustic.

There can therefore be situations where the direct and reflected rays combine in phase, causing the sound pressure level to increase. The phenomenon of refraction is frequency dependent and changes with the wind direction. This effect is more pronounced when the ratio of acoustic wavelength to the radius of the curvature of the predicted path length is small. The frequency of sound at which the increase in the sound pressure level takes place (see Figures 15) decreases with the wind

direction angle. This makes sense, because the greater this angle, the greater the values of $R'_{1,2}$ and the lower the frequency at which the constructive interference can occur.

Given the above, the magnitude of this upwind propagation effect would be expected to vary from that shown when derived using in more complex models (e.g. those that include complex terrain profiles, atmospheric turbulence along the propagation path, variations in ground absorption at different ranges from the source etc.). Investigation using such models would enable the likely magnitude of the effect in practically encountered situations to be determined.

Apart from the foregoing effect, which is evident to varying degrees at differing distances in the results for all propagation directions from 90 degrees to 180 degrees, Figures 15 indicate that for distances greater than 625 m (where the attenuation suggested in the IoA GPG begins to take effect for the particular turbine hub height and rotor diameter considered in this paper) the IoA GPG method generally predicts noise levels that are higher than the GFPE model for the generic turbine considered.

The results of Figures 15 also lead to another possible source of amplitude modulation in the case of upwind sound propagation. This possibility arises due the varying horizontal distance at which the upwind acoustic shadow zone may occur for sources of differing heights. The potential for such upwind amplitude modulation effects was previously identified in [RenewableUK, 2012].

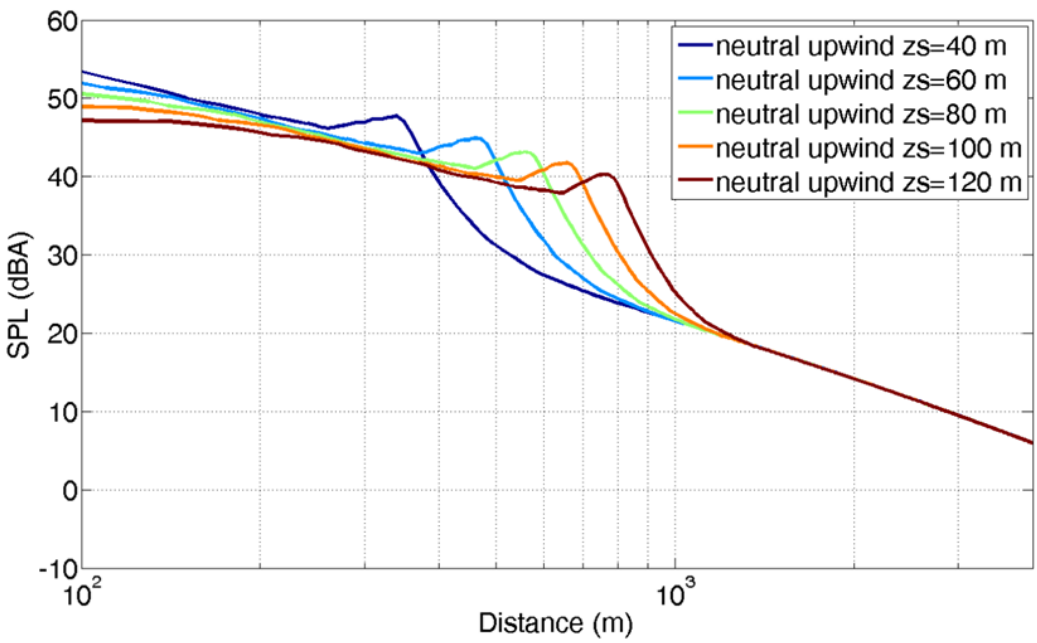

Figure 16 Predicted noise levels under upwind propagation with refraction in a neutral atmosphere for differing source heights.

Figure 16 shows the calculated noise levels as a function of upwind distance from sources modelled at each of the heights previously presented in Figure 12. Taking as an example the results corresponding to a source to receiver distance of 800 m, the received noise levels from the sources, all of which are assumed to have the same source level (see previous footnote 3), may vary between approximately 39 dB(A) for the 120 m height source to as low as approximately 24 dB(A) for the 40 m height source. Combining the relative contributions of the three sources corresponding to each of the two rotor positions shown in Figure 12 reveals that these shadow zone propagation effect would yield a variation in the overall received noise levels between the two extreme rotor positions of approximately 6.5 dB.

4. Conclusions and recommendations

This paper has considered the use of the Green's Function Parabolic Equation (GFPE) method to predict A-weighted noise levels from typical wind turbine noise sources. The results obtained have been compared to an engineering method of calculation commonly used in the UK (ISO 9613-2).

The results have been based on the characteristics of a generic turbine of 2 MW to 3 MW size with a tower height of 80 m and a rotor diameter of 90 m located on flat ground. The source has been consistently modelled as omnidirectional with a fixed sound power output in order to allow the study of propagation effects only in isolation from other factors, such as the extent to which meteorology may influence source levels and directivity.

The implementation of the GFPE method enables the relatively efficient calculation of overall A-weighted sound pressure level results in addition to frequency specific results. As such, the use of the GFPE potentially offers a practical means of supplementing the current preferential use of engineering methods of calculation for wind turbine noise propagation.

In general, the GFPE method applied to the modelled 80 m source height provides results that are consistent with, but typically slightly lower than, the ISO 9613-2 predictions. The predictions further indicate that propagation effects related to both ground properties and atmospheric stability conditions (unstable, neutral, stable) have little influence on the predicted noise levels. Whilst outside the scope of the present study, it is noted here that atmospheric stability could, however, be an important factor in controlling the source levels generated by wind turbines.

The influence of both ground properties and atmospheric stability conditions become increasingly significant for lower source heights.

The effect of considering separate noise sources on each of the turbine blades, rather than a single source concentrated at the turbine hub height, has also been examined. These calculations indicate that, in general, very little amplitude modulation in predicted noise levels at the blade rotation rate can be expected due to propagation effects at a distance of 1 km downwind from a wind turbine. As a consequence, reports of higher amplitude modulation at the blade rotation rate at such downwind locations are most likely related to source effects.

For the specific case of a stable atmosphere with downwind refraction, the GFPE model suggests that locally elevated noise levels at distances of approximately 1.5

km from the turbine could occur. This feature has been identified to arise specifically from the noise radiated from the portion of the blades as they pass the lowest point on their rotational path. The resultant effect could be to either increase or decrease amplitude modulation at the blade rotation rate, depending on the situation considered.

The foregoing observed feature, however, requires further study to establish to what degree its predicted occurrence is a function of the simplifying assumptions (most notably the simplification of the modelled turbulence, the assumed constant atmospheric and ground conditions with horizontal distance, and the flat ground profile) and therefore whether or not it would likely occur in practice and, if so, to what degree.

The effects of wind direction on received noise levels have also been modelled using the GFPE method. These results have been compared with predictions obtained using the ISO 9613-2 [ISO, 1996] method when applied in accordance with UK recommendations for the application of this standard to wind turbine noise [IoA, 2013]. The IoA recommendations include suggested corrections to allow for the expected variable attenuation when sound is propagating in an upwind direction from the turbines.

In general, with regard to the effects of wind direction, the IoA calculation method produces predictions that are higher than those produced by the GFPE model. This is apart from under upwind conditions where, and most notably for a generally narrow range of distances from between approximately 500 m and 800 m from the turbine and for the specific turbine dimensions considered in this paper, the GFPE model predicts higher noise levels not only when compared to the IoA method for the corresponding upwind direction, but also when compared with the corresponding calculated noise levels at those distances under downwind propagation conditions.

A physical explanation for the occurrence of the foregoing feature has been proposed. However, this explanation again highlights the fact that it may not be experienced to the same degree in practically encountered situations by reason of the simplifying assumptions used in the model, as discussed above. Further GFPE modelling work, in particular including a more detailed consideration of the effects of atmospheric turbulence, would be required to establish the likely practical occurrence of this upwind effect.

Finally, the potential effects of noise propagation on the degree of amplitude modulation at the blade rotation rate experienced at typical residential distances from a turbine have been investigated. Under downwind conditions it has been determined that very little modulation (of the order of just 0.1 dB) would be expected at a distance of 1 km due to propagation effects, but that source effects could introduce significant levels of modulation into the received noise levels at this distance

Under upwind propagation, at a worst case distance of 800 m from the turbine for the specific turbine dimensions considered in this paper, the GFPE model indicates that a peak to trough modulation depth at the blade rotation rate of approximately 6.5 dB could be experienced due to propagation effects alone.

Further work is required to establish whether the above conclusions, and particularly those relating to specific isolated effects, would still hold for practically encountered and more complex scenarios including, but not restricted to:

- more detailed consideration of atmospheric turbulence along the propagation path;
- ground absorption that varies with range (e.g. for the case of propagation over inland bodies of water, or for propagation from offshore sources to onshore receivers);
- non-flat terrain profiles, including both topographic scale variations in height and local perturbations;
- temporal, spectral and directivity effects in the noise emitted by wind turbines;
- the interpretation of results accounting for the spectral content of the received noise levels.

It should also be recognised that the focus of this paper has been to compare and contrast predictions made using the GFPE method against the engineering method commonly used in the UK and, as such, no comparison between measured and predicted noise levels has been made. Whilst such comparisons have previously been carried out in relation to measured wind turbine noise levels and those predicted using the ISO 9613 method [Cooper and Evans, 2013], further work would be required to establish the accuracy of the GFPE method as compared to measured noise levels when applied to wind turbine noise in real-world scenarios.

References

Attenborough, A., Li, K. M. and Horoshenkov, K. V. (2007) Predicting Outdoor Sound, Taylor and Francis.

Cooper, J. and Evans, T. (2013) Accuracy of noise predictions for wind farms, 5th International Conference on Wind Turbine Noise, Denver, 28-30 August 2013

Cooper,J, Evans, T. and Alamshah, V (2014) Influence of non-standard atmospheric conditions on turbine noise levels near wind farms, Internoise 2014, Melbourne, Australia.

Delany, M.E. and Bazley, E.N. (1970) Acoustical Properties of Fibrous Absorbent Materials," Appl. Acoust. 3, 105-116.

Dyer, A.J. (1994) A review of flux-profile relations, Bound. Layer Meteor. 1, 363-372.

IoA GPG (2013) Institute of Acoustics, A Good Practice Guide to the Application of ETSU-R-97 for the Assessment and Rating of Wind Turbine Noise.

Forssén, J. Schiff, M., Pedersen, E., Persson, K. (2010) Waye, Wind Turbine Noise Propagation over Flat Ground: Measurements and Predictions Acta Acustica united with Acustica 96(4): 753-760.

Gilbert, K., Di, X. (1993) A fast Green's function method for one-way sound propagation in the atmosphere. J. Acoust. Soc. Am. 94 (1993) 2343-2352.

Holtslag, A.A.M., Estimates of diabatic wind speed profiles from nearsurface weather observations, Boundary-Layer Meteorol. 29, 225-250 (1984).

International Electrotechnical Commission. IEC 61400-11, Wind Turbine Generator Systems – Part 11: Acoustic Noise Measurement Techniques, 2013

Institute of Acoustics (2013) A Good Practice Guide to the Application of ETSU-R-97 for the Assessment and Rating of Wind Turbine Noise, May 2013

ISO 9613-2 (1996) International Standards Organization. Acoustics -- Attenuation of sound during propagation outdoors -- Part 2: General method of calculation

Kaliski, K., Wilson, D. K., Vecherin, S., and Duncan, E. (2011) Improving Predictions of Wind Turbine Noise Using PE Modeling. Presented at NOISE-CON 2011 - Institute of Noise Control Engineers, Portland, OR.

Leventhall G and Bowdler D (2011) Wind Turbine Noise - How it is produced, propagated measured and received - Chapter 3, Multi-Science Publishing, ISBN 978-1-907132-30-8

Li, K. M. (1996), Propagation of sound above an impedance plane in a downward refracting atmosphere, J. Acoust. Soc. Am., 99:746–754.

Nota, R. Barelds, D. van Maercke (2005) Engineering method for road traffic and railway noise after validation and finetuning. Technical Report HAR32TR-040922-DGMR20, Harmonoise WP3.

Oerlemans, S. and Schepers, G. (2009), Prediction of Wind Turbine Noise Directivity and Swish, Third International Meeting on Wind Turbine Noise, Aalborg Denmark, 17 – 19 June 2009.

Oerlemans, S. (2011). An explanation for enhanced amplitude modulation of wind turbine noise, Netherlands National Aerospace Laboratory (NLR), report NLR-CR-2011-071.

Plovsing, B., Søndergaard, B., (2011) Wind turbine noise propagation: Comparison of measurements and predictions by a method based on geometrical ray theory, Noise Control Engineering Journal, 59(1): 10-22.

Raspet, R. and Wu, W., (1995) Calculation of average turbulence effects on sound propagation based on the fast field program formulation, J. Acoust. Soc. Am., 97:147–153.

RenewableUK, (2013) Wind Turbine Amplitude Modulation: Research to Improve Understanding as to its Cause and Effect, Dec 2013

Salomons, E., van Maercke, D., Defrance, J., de Roo, F., (2011) The Harmonoise Sound Propagation Model Source: Acta Acustica united with Acustica, 97(1), 62-74.

Salomons, E. (1998) Improved Green’s function parabolic equation method for atmospheric sound propagation. J. Acoust. Soc. Am. 104, 100-111.

Salomons, E.M. (2001) Computational Atmospheric Acoustics, Springer.